Turbulence, Heat and Mass Transfer 9

Effect of Stefan flow on drag coefficient of reactive spherical particles in gas flow

T. Jayawickrama[1], N.E.L. Haugen[2], M.U. Babler[3] and K. Umeki[1]

[1]*Division of Energy Sciences, Luleå University of technology, SE-971 87 Luleå, Sweden. thamali.rajika.jayawickrama@ltu.se, kentaro.umeki@ltu.se*

[2]*SINTEF Energy Research, N-7465 Trondheim, Norway. nils.e.haugen@sintef.no*

[3]*Department of Chemical Engineering, KTH Royal Institute of Technology, SE-100 44 Stockholm, Sweden. babler@kth.se*

Abstract — Particle laden flows with reactive particles are common in industrial applications. Chemical reactions inside the particle or deposition at the surface can generate additional flow phenomena that affect the heat, mass and momentum transfer between the particle and bulk flow. This work aims at investigating the effect of Stefan flow on the drag coefficient of a spherical particle immersed in a uniform flow. Fully resolved 3D simulations were carried out for particle Reynolds numbers based on the free stream velocity ranging from 0.5 to 3. Simulations are carried out in *foam*-extend CFD software, using the Immersed Boundary(IB) method for treating fluid-solid interactions. The simulations were validated against data for particles without reactive flow, and against the analytical solution for Stefan flow around a particle in a quiescent fluid. We found that in the considered range of Reynolds number the drag coefficient decreases linearly with in increase in Stefan flow velocity.

1. Introduction

Many industrial applications involve particle laden flows with reactive particles, such as combustion of solid fuels, food processing, pollution control, etc. Unlike ordinary particle-laden flows, reacting particles exchange mass with surrounding bulk fluid. Stefan flow, induced by chemical reactions inside or at the surface of the particle, may have effects on gas-solid interactions, i.e. the momentum, heat and mass transfer between the particle and the bulk flow. Stefan flow caused by chemical reactions is especially pronounced in gasification and combustion processes, where, upon being released into the hot environment, the fuel particles undergo fast devolatilization resulting in a pronounced gas stream leaving the particle. Several studies considered the effect of Stefan flow on the mass transfer coefficient for combustion of solid particles (Kalinchak, 2001; Yu et al., 2013). However, only few studies addressed the effect of Stefan flow on the drag coefficient (Renksizbulut and Yuen, 1983; Farazi et al., 2016). The correlations proposed in these works are specific for the studied conditions, and derived empirically without considering the change in flow fields due to the Stefan flow.

This study investigates how Stefan flow affects the interaction between gas flow and reacting particle, aiming at developing a model describing the change of drag coefficient due to Stefan flow in iso-thermal fluid flow. Resolved numerical simulation were carried out for a flow surrounding a stationary particle with outgoing/incoming flow. The Reynolds(Re) numbers of the flow were selected based on particle size range, slip velocity and temperature range of the flow in entrained-flow gasification and pulverized combustion. Due to the unavailability of experimental data with Stefan flow, the results were validated with two separate sources: experimental data without Stefan flow and analytical solution of flow field with Stefan flow in a quiescent environment.

2. Methodology

The numerical simulations considered a single spherical particle immersed in a uniform isothermal flow. Entrained flow gasification and pulverized combustion were selected as possible application when selecting flow conditions. Three Re no.s were selected considering particle size (0.1-1.0 mm), slip velocity (<3 m s^{-1}), and gas properties (taken as nitrogen at 1400 K) typical for entrained flow gasification (Göktepe et al., 2016). The independence of drag coefficients from particle size and slip velocity was examined by using two combinations in the same Re no. The Stefan flow was considered as a constant flux from the particle surface. The magnitude of the mass flux was calculated from data during devolatilization and char conversion of biomass (Umeki et al., 2012). Generation and consumption of gas inside the solid phase were considered as a constant outgoing or incoming mass flux at the particle surface in normal direction.

Particle Re no was less than 20 in this study, meaning the flow is steady, axisymmetric and topologically similar (Johnson and Patel, 1999). Therefore, a quarter of the domain was simulated with symmetric boundaries. Tests for domain size and mesh refinement were carried out at the highest Re no. Eventually, we selected domain size and finest mesh at particle surface as $64D \times 32D \times 32D$ and $0.01D$, respectively.

Steady state simulations were carried out under isothermal conditions. The gas phase was assumed as incompressible. The discrete phase was described as a stationary, spherical particle without the change in size. The gas phase is governed by mass conservation,

$$\nabla.(\overrightarrow{u}) = 0, \tag{1}$$

and momentum conservation,

$$(\rho\overrightarrow{u}.\nabla)\overrightarrow{u} = -\nabla p + \mu\nabla^2\overrightarrow{u}. \tag{2}$$

where ρ is density of the fluid, $\overrightarrow{u}$ is velocity vector , p is pressure and μ is viscosity. Equations (1) and (2) were discretized with finite volume method using second-order schemes. The slip velocity between particle and bulk gas was expressed as a boundary condition of gas velocity at the inlet while Neumann boundary condition was applied at the outlet. Side walls of the domain was treated as slip walls.

The boundary at the particle surface was described using discrete forcing immersed boundary (IB) method .It uses the direct imposition of boundary conditions (Jasak et al., 2014) and the presence of the immersed surface/body is formulated through the boundary conditions. This boundary condition is depicted by interpolation/extrapolation of boundary data in to the closest fluid control volume (Fadlun et al., 2000). The used platform, *foam*-extend-3.2, uses quadratic interpolation (Jasak et al., 2014) for reconstruction of solid phase boundary conditions in to the closest fluid cells.

Drag coefficient was calculated as,

$$C_D = \frac{4(\overrightarrow{F}_{P,x} + \overrightarrow{F}_{viscous,x})}{\frac{1}{2}\rho U^2(\frac{\pi D^2}{4})}, \tag{3}$$

where ρ is density, U is slip velocity, and D is particle diameter. Pressure force, $\overrightarrow{F}_P$, and viscous force, $\overrightarrow{F}_{viscous}$, were calculated as,

$$\overrightarrow{F}_P = \sum(P_{sur} - P_{ref})S_{tri} \cdot \overrightarrow{n}, \qquad \overrightarrow{F}_{viscous} = \sum(\rho\nu S_{tri} \cdot \overrightarrow{n} \times \nabla\overrightarrow{U}) \tag{4}$$

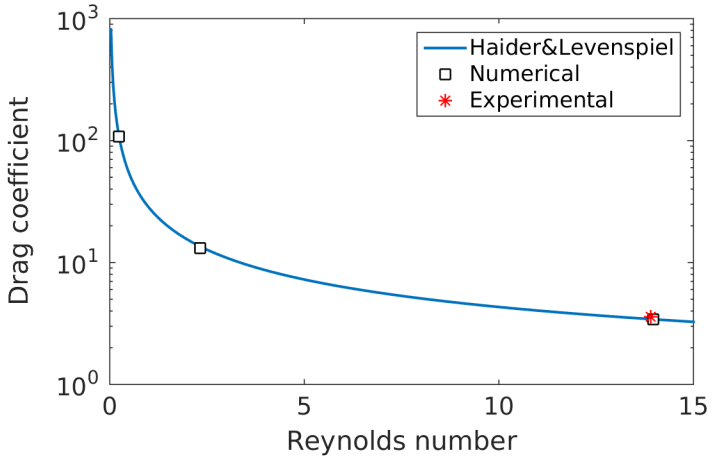

Figure 1: Drag coefficient as a function of Re no. Line: Correlation of (Haider and Levenspiel, 1989), symbols: numerical simulations and experiments.

where P_{sur} and P_{ref} are interpolated pressure at the particle surface and reference pressure, S_{tri} is surface area, $\overrightarrow{n}$ is normal direction, and ν is kinematic viscosity. Only the component in inlet flow direction was accounted for calculating total force as other components will be cancelled out due to symmetry of the flow.

3. Results and Discussion

Validation of simulations without Stefan flow is shown in Fig. 1. For the validation, three Re no.s were considered. The drag coefficient obtained from our simulations is in excellent agreement with the data reported in (Haider and Levenspiel, 1989). Simulations with Stefan flow only (particle in a stagnant fluid) showed a similarly good agreement with the analytical solution for this case.

Having validated our numerical simulation we studied the effect of Stefan flow. In all cases with and without Stefan flow, we found that the viscous force is higher than the pressure force (around twice of pressure force) as expected for low Re no.s. The pressure force turned out to be not affected by the Stefan flow and it is almost constant for a given Re no. On the contrary, the viscous force decreases with an outward Stefan flow and increases with an inward Stefan flow. Comparison of simulations data with and without Stefan flow shows an increase of the boundary layer thickness (shift outward) for outward Stefan flow and a decrease (shift inward) for inward Stefan flow. This can be understood as a pushing of the boundary layer away from the particle surface in case of an outward Stefan flow, respectively a pulling-in in case of an inward Stefan flow. This thickening of boundary layer will affect the reduction of the velocity gradient and then to the low viscous force. On the other hand, up stream side of the sphere can experience a higher velocity gradient due to the Stefan flow while downstream side experience a lower velocity gradient. The overall effect of low viscous force shows a higher impact from boundary layer thickening and downstream velocity gradient than up stream velocity gradient. Fig. 2 shows the normalized drag coefficient plotted against the normalized Stefan flow velocity at different Re no.s. The data indicates that the ratio between the drag coefficient with and without Stefan flow decreases faster the higher the Re no. For the highest Stefan flow velocity, and drag ratio reaches 0.7. This significant reduction in drag coefficients show the importance of considering Stefan flow in entrained flow gasification and pyrolysis combustion applications

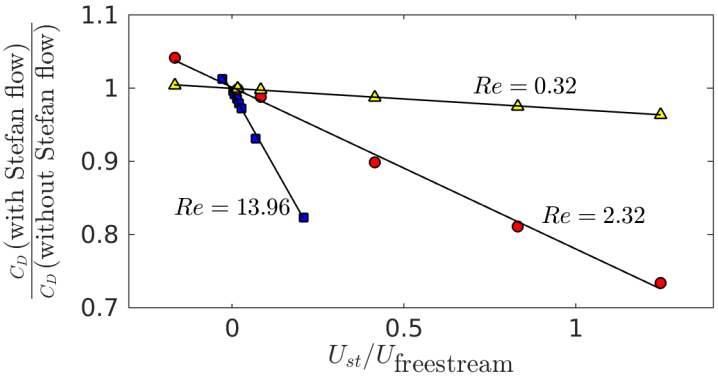

Figure 2: Normalized drag coefficient vs normalized Stefan flow velocity at different Reynolds numbers.

where the Re no range is applicable.

References

E. A. Fadlun, R. Verzicco, P. Orlandi, and J. Mohd-Yusof. Combined Immersed-Boundary Finite-Difference Methods for Three-Dimensional Complex Flow Simulations. *Journal of Computational Physics*, 161:35–60, 2000. doi: 10.1006.

S. Farazi, T. Sayadi, and H. Pitsch. Numerical analysis of the drag force acting on the reactive single char particle under oxy-fuel condition. *Proc. of the China National Symposium on Combustion 2016*, 2016.

B. Göktepe, A. H. Saber, R. Gebart, and T. S. Lundström. Cold flow experiments in an entrained flow gasification reactor with a swirl-stabilized pulverized biofuel burner. *International Journal of Multiphase Flow*, 85:267–277, 2016. ISSN 03019322. doi: 10.1016/j.ijmultiphaseflow.2016.06.016.

A. Haider and O. Levenspiel. Drag coefficient and terminal velocity of spherical and nonspherical particles. *Powder technology*, 58(1):63–70, 1989.

H. Jasak, D. Rigler, and Z. Tukovic. Design and implementation of Immersed Boundary method with discrete forcing approach for boundary conditions. *In proceed- ings of 6th European Congress on Computational Fluid Dynamics - ECFD VI*, 2014.

T. A. Johnson and V. C. Patel. Flow past a sphere up to a Reynolds number of 300. *J. Fluid Mech*, 378:19–70, 1999. doi: 10.1017/S0022112098003206.

V.V. Kalinchak. Influence of Stefan flow and convection on the kinetics of chemical reactions and heat and mass exchange of carbon particles with gases. *Journal of Engineering Physics and Thermophysics*, 74(2):323–330, 2001.

M. Renksizbulut and M. C. Yuen. Numerical Study of Droplet Evaporation in a High-Temperature Stream. *Journal of Heat Transfer*, 105(2):389–397, 1983. ISSN 00221481. doi: 10.1115/1.3245591.

K. Umeki, K. Kirtania, L. Chen, and S. Bhattacharya. Fuel Particle Conversion of Pulverized Biomass during Pyrolysis in an Entrained Flow Reactor. *Industrial & Engineering Chemistry Research*, 51:13973–13979, 2012. doi: 10.1021/ie301530j.

J. Yu, K. Zhou, and W. Ou. Effects of Stefan flow and CO oxidation on char particle combustion in O2/CO2 atmosphere. *Fuel*, 106:576–585, 2013. ISSN 00162361. doi: 10.1016/j.fuel.2013.01.005.